Accepted Manuscript

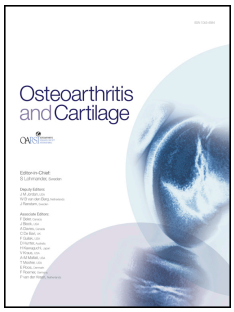

Subchondral bone in osteoarthritis: Association between MRI texture analysis and histomorphometry

Dr James W. MacKay, Dr Philip J. Murray, Mr Bahman Kasmai, Glyn Johnson, Professor, Simon T. Donell, Professor, Andoni P. Toms, Professor

PII: S1063-4584(16)30472-1

DOI: 10.1016/j.joca.2016.12.011

Reference: YJOCA 3914

To appear in: *Osteoarthritis and Cartilage*

Received Date: 1 August 2016

Revised Date: 14 November 2016

Accepted Date: 7 December 2016

Please cite this article as: MacKay JW, Murray PJ, Kasmai B, Johnson G, Donell ST, Toms AP, Subchondral bone in osteoarthritis: Association between MRI texture analysis and histomorphometry, *Osteoarthritis and Cartilage* (2017), doi: 10.1016/j.joca.2016.12.011.

TITLE:

SUBCHONDRAL BONE IN OSTEOARTHRITIS: ASSOCIATION BETWEEN MRI TEXTURE ANALYSIS AND HISTOMORPHOMETRY

MANUSCRIPT TYPE:

Full length original research article

AUTHORS:

Dr James W MacKay[1] james.mackay@nnuh.nhs.uk

Dr Philip J Murray[1] philip.murray@nnuh.nhs.uk

Mr Bahman Kasmai[1] bahman.kasmai@nnuh.nhs.uk

Professor Glyn Johnson[1,2] glyn.johnson@uea.ac.uk

Professor Simon T Donell[2,3] simon.donell@nnuh.nhs.uk

Professor Andoni P Toms[1,2] andoni.toms@nnuh.nhs.uk

[1]Department of Radiology, Norfolk & Norwich University Hospital, Norwich, UK

[2]Norwich Medical School, University of East Anglia, Norwich, UK

[3]Department of Trauma & Orthopaedics, Norfolk & Norwich University Hospital, Norwich, UK

CORRESPONDING AUTHOR:

Dr James MacKay
Radiology Academy
Cotman Centre
Norfolk & Norwich University Hospital
Colney Lane
Norwich NR4 7UB

Tel: +44 788 245 9094
Fax: +44 1603 286 146
Email: james.mackay@nnuh.nhs.uk

RUNNING TITLE:

MRI TEXTURE ANALYSIS OF SUBCHONDRAL BONE

ABSTRACT

Objective

Magnetic resonance imaging (MRI) texture analysis is a method of analyzing subchondral bone alterations in osteoarthritis (OA). The objective of this study was to to evaluate the association between MR texture analysis and ground-truth subchondral bone histomorphometry at the tibial plateau.

Design

The local research ethics committee approved the study. All subjects provided written, informed consent. This was a cross-sectional study carried out at our institution between February and August 2014.

Ten participants aged 57-84 with knee OA scheduled for total knee arthroplasty (TKA) underwent pre-operative MRI of the symptomatic knee at 3T using a high spatial- resolution coronal T1 weighted sequence. Tibial plateau explants obtained at the time of TKA underwent histological preparation to allow calculation of bone volume fraction (BV.TV), trabecular thickness (Tb.Th), trabecular separation (Tb.Sp) and trabecular number (Tb.N). Texture analysis was performed on the tibial subchondral bone of MRI images matched to the histological sections. Regression models were created to assess the association of texture analysis features with BV.TV, Tb.Th, Tb.Sp and Tb.N.

Results

MRI texture features were significantly associated with BV.TV (R^2 = 0.76), Tb.Th (R^2 = 0.47), Tb.Sp (R^2 = 0.75) and Tb.N (R^2 = 0.60, all $p < 0.001$). Simple grey-value histogram based texture features demonstrated the highest standardized regression coefficients for each model.

Conclusion

MRI texture analysis features were significantly associated with ground-truth subchondral bone histomorphometry at the tibial plateau.

KEYWORDS

Osteoarthritis; Magnetic resonance imaging; Subchondral bone; Texture analysis; Histomorphometry

INTRODUCTION

At present, efficacious disease modifying treatments for osteoarthritis (OA) are lacking [1]. Imaging has the potential to play an important role in the development of disease modifying treatments by assessing response to novel therapeutic approaches and improving understanding of OA natural history [2]. For this potential to be realized, sensitive and reliable imaging biomarkers are required. OA is considered as a disease of the entire joint, involving cartilage, bone, synovium, ligaments, menisci (for knee OA), capsule and juxta-articular muscle[3]. Much research interest has focused on assessment of cartilage, however it is also desirable to have reliable imaging biomarkers of other involved tissues such as the subchondral bone.

Texture analysis has been described as a method of analyzing subchondral bone on plain radiographs, computed tomography (CT) and magnetic resonance imaging (MRI) [4–6]. Texture analysis is a statistical method of analyzing an image or region of interest (ROI) based on the distribution and spatial organization of gray (pixel) values within it[7]. Its utility in the setting of subchondral bone analysis in OA lies in detecting and quantifying alterations in structure that are not detectable or difficult to quantify reliably using qualitative or alternative quantitative methods.

The current study focuses on MRI texture analysis at the knee. The advantages of using MRI for texture analysis over plain radiographs or CT are the cross-sectional nature of the images (compared to plain radiographs), the lack of

radiation exposure and the ability to assess other tissues involved in OA (particularly cartilage, synovium and meniscus) in a single examination.

MRI texture analysis has previously demonstrated significant differences in subchondral bone texture between controls and individuals with OA[8]. Alternative methods of assessing subchondral bone using MRI are available including direct estimation of microstructural parameters[9,10]. However, texture analysis has the advantages of the ability to use standard clinical sequences, the lack of need to binarize images using an arbitrary threshold, and superior discrimination ability between subjects with OA and controls[11].

One of the principal disadvantages of MRI texture analysis is the current lack of histological validation. It is important to assess the relationship between MRI texture analysis and ground-truth subchondral bone structure to establish the construct validity of this technique before it can be considered for use in further longitudinal or interventional studies. The histological gold standard for assessment of bone structure is the technique of histomorphometry which is the quantitative analysis of microscopic bone structure [12].

Thus, the purpose of this study was to evaluate the association between MRI texture analysis and ground-truth subchondral bone histomorphometry at the tibial plateau.

MATERIALS & METHODS

The local research ethics committee approved the study. All subjects provided written, informed consent. This was a cross-sectional study carried out at our institution between February and August 2014.

Participants

Ten participants (median age 70, range 57-84, 7 females) who were scheduled to undergo total knee arthroplasty (TKA) at our institution for primary OA of the knee were recruited at the time of their clinic visit immediately prior to TKA.

Participants were excluded if there was a history of significant ipsilateral lower limb injury, previous ipsilateral lower limb surgery, inflammatory arthritis, hematological malignancy, bone metastases, metabolic bone disease, or if there was a contraindication to MRI.

Participants had their height and weight recorded at the time of examination. All participants had recent AP weight bearing knee radiographs available (median 30 days previously, range 0 – 160 days). These were used to record the severity of medial and lateral tibiofemoral compartment OA using the Kellgren-Lawrence grading system[13]. Kellgren-Lawrence grading was performed by two radiology residents (JM & PM) with 3 years' experience. Participants completed an Oxford Knee Score questionnaire in order to assess severity of symptoms[14].

MRI acquisition

The knee scheduled for TKA of each participant was imaged using a dedicated 8-channel transmit/receive knee coil (Invivo, Gainseville, FL, USA) on a wide-bore 3.0 T platform (GE 750w, GE Healthcare, Amersham, UK). Sequences obtained included a 2D coronal T1 weighted sequence (FOV 12 × 12.3 cm, matrix 512 × 512, TR 593 ms, TE 17.65 ms, NEX 1, slice thickness 2.8 mm, slice gap 2.5 mm, sequence duration approximately 3 minutes) designed to maximize in-plane spatial resolution (0.23 x 0.24 mm) and signal-to-noise ratio for optimal assessment of subchondral bone (figure 1). The MRI examination was performed at the time of the participant's pre-operative assessment to ensure a short interval between MRI and TKA (median 13 days, range 6 – 29 days).

[FIGURE 1]

Bone specimens

The tibial plateau of each participant was removed as part of the TKA procedure as a single block of tissue. This was placed in 10% buffered formal saline for fixation and stored at room temperature while awaiting processing. Surgical sutures were used to identify the medial/lateral and anterior/posterior margins of the tibial plateau at the time of resection.

Histological processing involved dividing the tibial plateau in half in the sagittal plane into medial and lateral portions using a bone saw (Exakt Diament Band Saw, Exakt Advanced Technologies GmBH, Germany), to enable the samples to fit standard 30 x 25 mm histological cassettes. The central portion of the tibial

plateau specimens was then sectioned in the coronal plane (to match the orientation of the MRI images) using the bone saw with the location of the blocks taken recorded on a schematic diagram of the plateau. The tissue block then underwent decalcification, embedding in paraffin, cutting then staining with hematoxylin and eosin. The blocks were typically 30 mm in width and included between 5-10 mm in depth of tibial subchondral bone. Preparation of the blocks was supervised by an experienced bone pathologist.

Histomorphometry

Prepared histological blocks were converted to digital format using a high-resolution histological scanner (Hamamatsu Photonics, Welwyn Garden City, UK). The digital blocks were exported in TIFF format and analyzed using ImageJ (NIH, Bethesda, MD, USA).

For each sample, following calibration for magnification, regions of interest (ROI) were created to enclose the subchondral bone. ROIs were defined superiorly by the bone/cartilage interface, laterally/medially by the tibial spines and lateral/medial joint margin and inferiorly by the inferior limit of the specimen, which was typically 5 – 10 mm in depth in the coronal plane (figure 2).

ROIs were binarized by stretching the pixel intensity histogram of the region of interest to enhance contrast between trabeculae and marrow, with subsequent automatic thresholding into bone and non-bone pixels.

The standard histomorphometric parameters bone volume fraction (BV.TV), trabecular thickness (Tb.Th), trabecular separation (Tb.Sp) and trabecular

number (Tb.N) were then derived (figure 2). The calculation of these parameters has been described in depth previously[12]. In brief, BV.TV is the number of bone pixels divided by the total number of pixels in the ROI. Tb.Th was calculated using the Local Thickness ImageJ plugin by deriving the Euclidean distance map from the binarized image, removing redundant points to produce distance ridges, then by calculating the thickness at each point along the distance ridge[15]. Tb.N represents the number of trabeculae per unit length and is calculated as Tb.N = BV.TV/Tb.Th. Tb.Sp is subsequently calculated as Tb.Sp = (1/Tb.N) – Tb.Th.

[FIGURE 2]

MRI texture analysis

MRI images were manually matched to histology blocks using the schematic diagrams created at the time of sample processing. Topological features (e.g. osteophytes, bone contour) were used to aid the matching process (figure 3). The matching process was performed twice by a single observer (JM) and demonstrated excellent intra-observer reproducibility with a weighted kappa of 0.93 (95% confidence interval 0.89 – 0.97).

The matched MRI images (in the original Digital Imaging and Communications in Medicine (DICOM) format) were imported into a dedicated texture analysis program (MazDa v 4.6) for analysis[16]. We used default image compression settings of 4 bits/pixel for calculation of absolute gradient features, and 6 bits/pixel for calculation of gray-level co-occurrence matrix (GLCM) and run-length matrix (RLM) parameters. ROIs were created manually in the medial and

lateral subchondral bone to match those used for analysis of the histology blocks as closely as possible (figure 1). A total of 18 texture features were then generated for each ROI. These texture features were chosen as they had demonstrated significant differences between subjects with OA and controls in a previous study of subchondral bone texture in OA, suggesting that they may be useful to describe alterations occurring in the subchondral bone in OA[8]. Texture features belonged to one of four classes: gray-level histogram, absolute gradient, RLM and GLCM.

Gray-level histogram features are simple descriptors of the distribution of gray levels (i.e. pixel intensity values) in the ROI. Gradient, RLM and GLCM features are higher order descriptors of the spatial organization of pixels in the ROI. A more detailed overview of these parameters is available[17,18]. RLM parameters were calculated 4 times for each pixel (in the horizontal, vertical, 45^{o} and 135^{o} directions) and GLCM parameters were calculated 20 times for each pixel at a variety of pixel offsets ranging from 1 to 5 pixels. The mean value of each RLM and GLCM parameter for each pixel in all possible directions and pixel offsets was calculated and used for subsequent analyses.

Inter-observer reliability of the MRI texture analysis technique used in this study has been reported previously, with ICCs ranging from 0.41 – 0.99 (12 out of 18 parameters had ICC > 0.9)[11].

[FIGURE 3]

Statistical analysis

Descriptive statistics for each calculated histomorphometric parameter and MRI texture feature were generated. The relationship between MRI texture features and histomorphometric parameters was assessed using scatter plots (data not shown).

To determine the MRI texture features best associated with each of the 4 histomorphometric parameters (BV.TV, Tb.Th, Tb.Sp and Tb.N) we used all-subsets multiple regression. The number of included texture features was limited to 5, in keeping with standard practice of limiting the number of explanatory variables to $n/10$ (we had 54 histological blocks available for analysis – see *Results*) to avoid model overfitting. The subset of MRI texture features with the lowest Bayesian information criterion (a parsimony-adjusted measure of fit) was chosen for each parameter. We did not perform mixed effects modelling (including subject as a random effect) as preliminary analysis indicated that there was no significant model intercept variability (as assessed by ANOVA) between subjects for any histomorphometry parameter model.

The chosen subset of MRI texture features was then used to perform multiple linear regression modeling for each histomorphometric parameter. Goodness-of-fit was assessed using unadjusted and Stein-adjusted R-squared[19]. Relative contributions of each individual texture feature were assessed using unstandardized and standardized regression coefficients (B/β). Standard multiple regression diagnostics were performed to assess the quality of each model including assessing distribution of residuals, influential cases,

174 multicollinearity and independence of errors (assessed using the Durbin-Watson
175 test).

176 We used the $p < 0.05$ level for statistical significance of the models and individual
177 texture features. All analyses were performed using R version 3.1.2 for Mac[20].

178

RESULTS

Participants

Baseline characteristics of study subjects are provided in table 1.

[TABLE 1]

Histomorphometry

A total of 63 histological blocks were obtained (median 6 per subject, range 5-8). Nine histological blocks were excluded from analysis following review due to excessive slicing artefact, leaving a total of 54 blocks for analysis. Mean values for each histomorphometric parameter are provided in table 2

[TABLE 2]

MRI texture analysis

Mean values of each MRI texture feature, calculated from 54 ROIs matched to the histological blocks, are provided in table 3.

[TABLE 3]

The correlations between histomorphometric parameters and MRI texture features are summarized graphically in figure 4.

[FIGURE 4]

Statistical analysis

Detailed multiple regression model summaries are provided in table 4.

198 For BV.TV, the MRI texture features selected using all-subsets regression were
199 the histogram mean, variance and skewness and the GLCM entropy and inverse
200 difference moment, with the final model adjusted $R^2 = 0.76$, $p<0.001$.

201 For Tb.Th, the features selected were the histogram mean, variance and skewness
202 and the RLM gray-level non-uniformity (GLNU), with the final model adjusted R^2
203 $= 0.47$, $p<0.001$.

204 For Tb.Sp, the features selected were the histogram mean and variance, the mean
205 absolute gradient, the GLCM contrast and the RLM run-length non-uniformity
206 (RLNU), with the final model adjusted $R^2 = 0.75$, $p<0.001$.

207 For Tb.N, the features selected were the histogram mean, the absolute gradient
208 variance and the RLM GLNU, with the final model adjusted $R^2 = 0.60$, $p<0.001$.

209 All models met the assumptions of homoscedasticity, independence of errors,
210 normally distributed residuals and no multicollinearity.

211 [TABLE 4]

212

DISCUSSION

This study demonstrates that MRI texture analysis features are significantly associated with ground-truth subchondral bone histomorphometry. This provides construct validation of MRI texture analysis and supports its use in further studies of subchondral bone in OA.

The subchondral bone of study participants at the medial tibial plateau demonstrated a higher bone volume and smaller number of widely spaced, thickened trabeculae (higher Tb.Th, higher Tb.Sp and lower Tb.N) when compared to normal tibial subchondral bone, in keeping with previous studies describing alterations in subchondral bone histomorphometry in OA[21]. The lateral tibial subchondral bone demonstrated similar trends in Tb.Th, Tb.Sp and Tb.N but had lower BV.TV when compared to normal subjects. Given that the majority of participants had medial compartment predominant disease, this may reflect off-loading of the lateral compartment due to varus malalignment.

Texture analysis revealed that study participants had, in general, more heterogeneous, less spatially organized subchondral bone when compared to values described in normal subjects[8]. For example, the variance of the signal intensity values within the subchondral ROIs was higher in study subjects, indicating greater heterogeneity, and absolute gradient and RLM non-uniformity parameters were lower, indicating fewer transitions between areas of high and low signal as are seen with normal the fine, linear subchondral trabeculae of normal subchondral bone.

The texture analysis feature for each histomorphometric parameter with the highest standardized regression coefficient (i.e. the most important to the model) was the simplest texture feature, the mean gray value of the ROI. Moreover, all models with the exception of Tb.N contained more than one simple histogram feature. While higher order texture features provide additional information on spatial organization and have shown statistically significant differences between subjects with OA and controls, our results suggest that they contribute relatively less in terms of association with histomorphometry.

A lower mean gray value was associated with higher BV.TV and Tb.Th but lower Tb.Sp and Tb.N. These histomorphometric changes are similar to the typical structural abnormalities seen in osteoarthritic subchondral bone[21]. Subchondral bone with higher BV.TV and thicker trabeculae is the histological correlate of subchondral sclerosis, a radiographic hallmark of OA[22]. On MRI, these areas of sclerosis appear as areas of low signal intensity and thus have a lower mean gray value.

Increased histogram variance was associated with higher BV.TV and Tb.Th, and lower Tb.Sp. The histogram variance can be thought of as the simplest measure of heterogeneity within the ROI. This suggests that in more 'osteoarthritic' bone, where the BV.TV and Tb.Th are higher, the heterogeneity and therefore histogram variance will be greater.

Higher order parameters contributing to the final models included the RLM parameters GLNU and RLNU and the GLCM parameter entropy which are indices of disorganization within the MRI image ROI. In general, the texture features

with the closest conceptual links to heterogeneity and organization are those that were most associated with histomorphometric parameters in the final models.

This study builds on previous work using MRI texture analysis and will aid future research in this area with regard to selection of texture features most likely to be most useful, taking into account discriminatory ability, reliability, and relationship to ground-truth structural parameters.

There is increasing recognition of the importance of subchondral bone in OA, together with the need for robust imaging biomarkers of joint structures other than cartilage[2,23]. There is evidence that changes in subchondral bone occur very early in the disease process, possibly preceding macroscopic cartilage degeneration. Subchondral bone is a dynamic tissue, capable of modeling and remodeling in response to changing load conditions (as per Wolff's law) and is therefore a therapeutic target of interest for potential disease modifying OA drugs (DMOADs) [24–26]. There is therefore the need for sensitive imaging biomarkers of subchondral bone. MRI texture analysis is one technique which has demonstrated the potential to meet this need, and now be considered for use in further studies.

Previous studies have demonstrated differences in subchondral bone texture between subjects with OA and controls using a variety of imaging modalities[4,27,28]. However, to our knowledge no previous study has sought to validate the technique using histomorphometry. We believe that this study's findings of associations between texture features and histomorphometry support the continued use of texture analysis in this setting.

A number of different approaches to texture analysis have been described with no one generally accepted analytic approach. One of the advantages of this study is the use of freely available texture analysis software which permits the use of a standardized approach between studies and increases the likelihood of results being replicated elsewhere. "Texture analysis" of bone has been used as a descriptor for a number of techniques. In the present study we have focused on statistical texture features (sometimes called Haralick texture, named after the researcher who first described the technique), which is distinct to other "texture" techniques such as direct estimation of bone microstructure and fractal signature analysis[17].

Our method involves 2D rather than 3D analysis, using statistical texture features as a surrogate measure of bone structure. While this has the disadvantage when compared to 3D analysis of not providing the opportunity to estimate structural parameters from MR images directly, advantages of 2D analysis include the ability to use higher SNR 2D spin echo images which have less susceptibility artefact at the bone/marrow interface when compared to the 3D gradient echo images required for 3D analysis, and the lack of requirement for arbitrary segmentation of subchondral bone into bone and non-bone voxels[11,29].

2D analysis of subchondral bone has also previously been performed on knee radiographs, primarily using fractal signature analysis (FSA) but also using dual x-ray absorptiometry (DXA) to assess subchondral bone mineral density. These techniques have shown the ability to discriminate between osteoarthritic and normal subchondral bone, and have good predictive validity for knee OA

304 progression[4,30–36]. Advantages of analyzing subchondral bone on plain
305 radiographs or DXA (compared with MRI) include the low cost and widespread
306 availability of these modalities, as well as the simplicity and speed of analyzing a
307 single 2D image. In addition, at present the predictive validity of subchondral
308 bone alterations as assessed MRI are less clear than for those assessed by plain
309 radiographs/DXA. Some studies have demonstrated the association between MRI
310 measurements such as subchondral bone size and bone shape and outcomes
311 including progression in radiographic disease, changes in MRI cartilage volume,
312 progression of clinical symptoms and the need for TKA[37,38]. However, there have
313 been conflicting findings in studies using alternative techniques, for example
314 semiquantitative MRI grading of subchondral sclerosis[39].

315 Nevertheless, assessing subchondral bone on MRI has the advantage over plain
316 radiographs of simultaneously allowing assessment of multiple aspects of
317 subchondral bone in a single examination, for example bone texture, bone shape,
318 and bone marrow lesions, as well as allowing assessment of other joint tissues
319 involved in OA. MRI texture analysis is likely to be less dependent on positioning
320 than radiographic texture analysis due to the radiographic depiction of multiple
321 overlapping trabeculae compared with the cross-sectional nature of MRI. Some
322 methods of MRI assessment of subchondral bone have demonstrated greater
323 sensitivity to change when compared with plain radiographs[40]. At present, there
324 has been no head-to-head comparison of texture analysis on plain radiographs
325 and MRI.

We believe that the technique used in this study should be viewed as complementary to techniques previously used for subchondral bone assessment, and has the ability to contribute to this active area of research.

There are several important limitations of this study. First, only 10 participants were included, limiting study power. Due to this small number of participants, data from the 7 female and 3 male participants were pooled for analysis. This approach ignores differences in histomorphometric parameters related to gender which are likely to be present, particularly given the postmenopausal status of female participants. All participants in the study had severe OA warranting TKA. While such a population was necessary to obtain tibial plateau explants for histomorphometry, it does mean that the study sample is biased towards more severe OA. The performance of our models in subjects with earlier stages of OA is therefore not clear.

The study was performed in a single center, at a single timepoint, thus limiting the generalizability of results. The sensitivity of MRI texture analysis to different acquisition parameters has been described previously, although with appropriate calibration the discrimination ability of texture features may be maintained[41,42]. The MRI analysis technique featured manual registration with histological blocks and manual ROI creation. Although this and other texture analysis techniques involving manual ROI creation have previously demonstrated good reliability, it is possible that automation or semi-automation may enhance this further and encourage a standardized approach between centers[43,44]. Finally, we used all-subsets regression to create our models. Automatic methods of variable selection

such as this have been criticized as causing problems with overfitting[45]. However, this is generally less of a problem than with alternative stepwise methods of variable selection, and we have attempted to minimize the risk of overfitting by limiting the number of model variables to *n*/10.

In conclusion, MRI texture features were significantly associated with ground-truth subchondral bone histomorphometry. This supports the use of MRI texture analysis as a valid technique for the assessment of subchondral bone structural alterations in OA.

ACKNOWLEDGEMENTS

The research team acknowledges the support of the National Institute for Health Research, through the Comprehensive Clinical Research Network. We thank Angela Bullough and Sue Butters, Orthopaedic Research Nurses, for their assistance with participant screening and recruitment. We thank Dr Tim Barker and Dr Lazslo Igali for supervising the preparation of the histological blocks and their assistance with this section of the *Methods*. No writing assistance was used.

AUTHOR CONTRIBUTIONS

Conception and design:	JM, GJ, SD, AT
Analysis and interpretation of the data:	JM, PM, BK
Drafting of the article:	JM, PM
Critical revision of the article:	BK, GJ, SD, AT
Final approval of the article:	JM, PM, BK, GJ, SD, AT
Provision of study materials or patients:	GJ, SD
Statistical expertise:	JM, AT
Obtaining of funding:	JM, AT
Administrative, technical, or logistic support:	PM, BK, GJ
Collection and assembly of data:	JM, PM

Guarantors of entire study: Dr James MacKay (james.mackay@nnuh.nhs.uk), Professor Andoni Toms (andoni.toms@nnuh.nhs.uk)

DECLARATION OF FUNDING AND ROLE OF FUNDING SOURCE

This study was funded by the Royal College of Radiologists via the Pump Priming Grant scheme. The funder had no role in the study design, data collection and analysis, preparation of the manuscript or the decision to submit the manuscript for publication.

COMPETING INTERESTS STATEMENT

The authors of this manuscript declare no relationships with any companies whose products or services may be related to the subject matter of the article.

REFERENCES

1. Hunter DJ. Pharmacologic therapy for osteoarthritis--the era of disease modification. *Nat Rev Rheumatol*. 2011;7(1):13-22. doi:10.1038/nrrheum.2010.178.

2. Hunter DJ, Altman RD, Cicuttini F, et al. OARSI Clinical Trials Recommendations: Knee imaging in clinical trials in osteoarthritis. *Osteoarthritis Cartilage*. 2015;23(5):698-715. doi:10.1016/j.joca.2015.03.012.

3. Hunter DJ, Felson DT. Osteoarthritis. *BMJ*. 2006;332(7542):639-642.

4. Hirvasniemi J, Thevenot J, Immonen V, et al. Quantification of differences in bone texture from plain radiographs in knees with and without osteoarthritis. *Osteoarthritis Cartilage*. 2014;22(10):1724-1731. doi:10.1016/j.joca.2014.06.021.

5. Link TM, Majumdar S, Lin JC, et al. Assessment of trabecular structure using high resolution CT images and texture analysis. *J Comput Assist Tomogr*. 1998;22(1):15-24.

6. Harrison LCV, Nikander R, Sikiö M, et al. MRI texture analysis of femoral neck: Detection of exercise load-associated differences in trabecular bone. *J Magn Reson Imaging*. 2011;34(6):1359-1366. doi:10.1002/jmri.22751.

7. Castellano G, Bonilha L, Li LM, Cendes F. Texture analysis of medical images. *Clin Radiol*. 2004;59(12):1061-1069. doi:10.1016/j.crad.2004.07.008.

8. MacKay JW, Murray PJ, Kasmai B, Johnson G, Donell ST, Toms AP. MRI texture analysis of subchondral bone at the tibial plateau. *Eur Radiol*. 2016;26(9):3034-3045. doi:10.1007/s00330-015-4142-0.

9. Lo GH, Tassinari AM, Driban JB, et al. Cross-sectional DXA and MR measures of tibial periarticular bone associate with radiographic knee osteoarthritis severity. *Osteoarthritis Cartilage*. 2012;20(7):686-693. doi:10.1016/j.joca.2012.03.006.

10. Schneider E, Lo GH, Sloane G, et al. Magnetic resonance imaging evaluation of weight-bearing subchondral trabecular bone in the knee. *Skeletal Radiol*. 2011;40(1):95-103. doi:10.1007/s00256-010-0943-z.

11. MacKay JW, Murray PJ, Low SBL, et al. Quantitative analysis of tibial subchondral bone: Texture analysis outperforms conventional trabecular microarchitecture analysis. *J Magn Reson Imaging*. 2016;43(5):1159-1170. doi:10.1002/jmri.25088.

12. Parfitt AM, Drezner MK, Glorieux FH, et al. Bone histomorphometry: standardization of nomenclature, symbols, and units. Report of the ASBMR

Histomorphometry Nomenclature Committee. *J Bone Miner Res*. 1987;2(6):595-610. doi:10.1002/jbmr.5650020617.

13. Kellgren JH, Lawrence JS. Radiological assessment of osteo-arthrosis. *Ann Rheum Dis*. 1957;16(4):494-502.

14. Dawson J, Fitzpatrick R, Murray D, Carr A. Questionnaire on the perceptions of patients about total knee replacement. *J Bone Joint Surg Br*. 1998;80-B(1):63-69.

15. Dougherty R, Kunzelmann K-H. Computing Local Thickness of 3D Structures with ImageJ. *Microsc Microanal*. 2007;13(Supplement S02):1678–1679. doi:10.1017/S1431927607074430.

16. Szczypiński PM, Strzelecki M, Materka A, Klepaczko A. MaZda--a software package for image texture analysis. *Comput Methods Programs Biomed*. 2009;94(1):66-76. doi:10.1016/j.cmpb.2008.08.005.

17. Haralick R, Shanmugam K, I Dinstein. Textural features for image classification. *IEEE Trans Syst Man Cybern*. 1973;3(6):610-621.

18. Tang X. Texture information in run-length matrices. *Image Process IEEE Trans On*. 1998;7(11):1602–1609.

19. Stevens JP. Model validation. In: Applied Multivariate Statistics for the Social Sciences, Stevens JP. New York: Taylor & Francis 2009:93-98.

20. R Core Team. *R: A Language and Environment for Statistical Computing*. Vienna, Austria: R Foundation for Statistical Computing; 2014. http://www.R-project.org.

21. Bobinac D, Spanjol J, Zoricic S, Maric I. Changes in articular cartilage and subchondral bone histomorphometry in osteoarthritic knee joints in humans. *Bone*. 2003;32(3):284-290.

22. Altman RD, Gold GE. Atlas of individual radiographic features in osteoarthritis, revised. *Osteoarthritis Cartilage*. 2007;15:A1-A56. doi:10.1016/j.joca.2006.11.009.

23. Funck-Brentano T, Cohen-Solal M. Subchondral bone and osteoarthritis: *Curr Opin Rheumatol*. 2015;27(4):420-426. doi:10.1097/BOR.0000000000000181.

24. Goldring MB, Goldring SR. Articular cartilage and subchondral bone in the pathogenesis of osteoarthritis. *Ann N Y Acad Sci*. 2010;1192:230-237. doi:10.1111/j.1749-6632.2009.05240.x.

25. Goldring MB, Berenbaum F. Emerging targets in osteoarthritis therapy. *Curr Opin Pharmacol*. 2015;22:51-63. doi:10.1016/j.coph.2015.03.004.

26. Kwan Tat S, Lajeunesse D, Pelletier J-P, Martel-Pelletier J. Targeting subchondral bone for treating osteoarthritis: what is the evidence? *Best Pract Res Clin Rheumatol*. 2010;24(1):51-70. doi:10.1016/j.berh.2009.08.004.

27. Wolski M, Podsiadlo P, Stachowiak GW, Lohmander LS, Englund M. Differences in trabecular bone texture between knees with and without radiographic osteoarthritis detected by directional fractal signature method. *Osteoarthritis Cartilage*. 2010;18(5):684-690. doi:10.1016/j.joca.2010.01.002.

28. Marques J, Genant HK, Lillholm M, Dam EB. Diagnosis of osteoarthritis and prognosis of tibial cartilage loss by quantification of tibia trabecular bone from MRI. *Magn Reson Med*. 2013;70(2):568-575. doi:10.1002/mrm.24477.

29. Majumdar S, Newitt D, Jergas M, et al. Evaluation of technical factors affecting the quantification of trabecular bone structure using magnetic resonance imaging. *Bone*. 1995;17(4):417-430. doi:10.1016/S8756-3282(95)00263-4.

30. Lespessailles E, Jennane R. Assessment of bone mineral density and radiographic texture analysis at the tibial subchondral bone. *Osteoporos Int*. 2012;23 Suppl 8:S871-876. doi:10.1007/s00198-012-2167-7.

31. Kraus VB, Feng S, Wang S, et al. Trabecular morphometry by fractal signature analysis is a novel marker of osteoarthritis progression. *Arthritis Rheum*. 2009;60(12):3711-3722. doi:10.1002/art.25012.

32. Woloszynski T, Podsiadlo P, Stachowiak GW, Kurzynski M, Lohmander LS, Englund M. Prediction of progression of radiographic knee osteoarthritis using tibial trabecular bone texture. *Arthritis Rheum*. 2012;64(3):688-695. doi:10.1002/art.33410.

33. Podsiadlo P, Dahl L, Englund M, Lohmander LS, Stachowiak GW. Differences in trabecular bone texture between knees with and without radiographic osteoarthritis detected by fractal methods. *Osteoarthritis Cartilage*. 2008;16(3):323-329. doi:10.1016/j.joca.2007.07.010.

34. Messent EA, Ward RJ, Tonkin CJ, Buckland-Wright C. Tibial cancellous bone changes in patients with knee osteoarthritis. A short-term longitudinal study using Fractal Signature Analysis. *Osteoarthritis Cartilage*. 2005;13(6):463-470. doi:10.1016/j.joca.2005.01.007.

35. Bruyere O, Genant H, Kothari M, et al. Longitudinal study of magnetic resonance imaging and standard X-rays to assess disease progression in osteoarthritis. *Osteoarthritis Cartilage*. 2007;15(1):98-103. doi:10.1016/j.joca.2006.06.018.

36. Cao Y, Stannus OP, Aitken D, et al. Cross-sectional and longitudinal associations between systemic, subchondral bone mineral density and knee cartilage thickness in older adults with or without radiographic

osteoarthritis. *Ann Rheum Dis*. 2014;73(11):2003-2009. doi:10.1136/annrheumdis-2013-203691.

37. Hunter D, Nevitt M, Lynch J, et al. Longitudinal validation of periarticular bone area and 3D shape as biomarkers for knee OA progression? Data from the FNIH OA Biomarkers Consortium. *Ann Rheum Dis*. 2016;75(9):1607-1614. doi:10.1136/annrheumdis-2015-207602.

38. Ding C, Cicuttini F, Jones G. Tibial subchondral bone size and knee cartilage defects: relevance to knee osteoarthritis. *Osteoarthritis Cartilage*. 2007;15(5):479-486. doi:10.1016/j.joca.2007.01.003.

39. Crema MD, Cibere J, Sayre EC, et al. The relationship between subchondral sclerosis detected with MRI and cartilage loss in a cohort of subjects with knee pain: the knee osteoarthritis progression (KOAP) study. *Osteoarthritis Cartilage*. 2014;22(4):540-546. doi:10.1016/j.joca.2014.01.006.

40. Bowes MA, Vincent GR, Wolstenholme CB, Conaghan PG. A novel method for bone area measurement provides new insights into osteoarthritis and its progression. *Ann Rheum Dis*. 2015;74(3):519-525. doi:10.1136/annrheumdis-2013-204052.

41. Collewet G, Strzelecki M, Mariette F. Influence of MRI acquisition protocols and image intensity normalization methods on texture classification. *Magn Reson Imaging*. 2004;22(1):81-91. doi:10.1016/j.mri.2003.09.001.

42. Mayerhoefer ME, Szomolanyi P, Jirak D, Materka A, Trattnig S. Effects of MRI acquisition parameter variations and protocol heterogeneity on the results of texture analysis and pattern discrimination: an application-oriented study. *Med Phys*. 2009;36(4):1236-1243.

43. Suoranta S, Holli-Helenius K, Koskenkorva P, et al. 3D Texture Analysis Reveals Imperceptible MRI Textural Alterations in the Thalamus and Putamen in Progressive Myoclonic Epilepsy Type 1, EPM1. *PLoS ONE*. 2013;8(7):e69905. doi:10.1371/journal.pone.0069905.

44. Hodgdon T, McInnes MDF, Schieda N, Flood TA, Lamb L, Thornhill RE. Can Quantitative CT Texture Analysis be Used to Differentiate Fat-poor Renal Angiomyolipoma from Renal Cell Carcinoma on Unenhanced CT Images? *Radiology*. 2015;276(3):787-796. doi:10.1148/radiol.2015142215.

45. Babyak MA. What you see may not be what you get: a brief, nontechnical introduction to overfitting in regression-type models. *Psychosom Med*. 2004;66(3):411-421.

FIGURE LEGENDS

Figure 1. Sample coronal T1w MR image

White dashed line outlines typical region of interest (ROI) placement. Note lower signal in medial tibial ROI.

Figure 2. Histological analysis

Digitized histology blocks (A) were enhanced using a histogram stretching algorithm (B) and were subsequently automatically binarized (C). This allowed estimation of BV.TV. Further processing using ImageJ's Local Thickness plugin (D) allowed calculation of Tb.Th. Tb.N and Tb.Sp were then calculated using these parameters.

Figure 3. Matched MR and histology images at (top row) medial and (bottom row) lateral tibial plateau

Note area of homogeneous low signal on MR (white arrowheads) corresponds to an area of trabecular thickening on histology (black arrowheads).

Figure 4. Correlation plot of histomorphometric parameters with MR texture features.

Strength and direction of correlation (Pearson's *r*) between texture features (horizontal axis) and histomorphometric parameters (vertical axis) is color coded according to the bar below the plot. Abbreviations are as per table 3.

TABLES

Table 1. Baseline characteristics of study subjects

Variable	Value
Age	70 (57 – 84)*
Body mass index (kg/m^2)	31.5 (25.2 – 40.9)*
Females/males	7/3
Left/right knee	4/6
Kellgren-Lawrence grade medial (0/1/2/3/4)	0/0/1/5/4
Kellgren-Lawrence grade lateral (0/1/2/3/4)	0/5/4/0/1
Oxford Knee Score†	18 (10 – 25)*

*Values presented are median (range).
†Range 0 – 48, with lower scores indicating more severe symptoms.

Table 2. Descriptive statistics for histomorphometric parameters

Parameter	**Mean (SD)**	
	Medial tibia	Lateral Tibia
BV.TV (%)	42 (10)	25 (7)
Tb.Th (μm)	339 (77)	253 (55)
Tb.Sp (μm)	487 (157)	795 (205)
Tb.N (1/mm)	1.24 (0.2)	0.99(0.2)

Abbreviations: BV.TV – bone volume fraction, Tb.Th – trabecular thickness, Tb.Sp – trabecular separation, Tb.N – trabecular number

Table 3. Descriptive statistics for MR texture features

Parameter	**Mean (SD)**	
	Medial tibia	Lateral Tibia
Histogram		
Mean	1862 (699)	3107 (930)
Variance*	4.82 (2.25)	6.98 (4.44)
Skewness	-0.36 (0.47)	-0.85 (0.47)
Absolute Gradient		
GrMean	1.04 (0.28)	1.21 (0.32)
GrVariance	0.51 (0.12)	0.70 (0.24)
GrSkewness	0.22 (0.20)	0.65 (0.43)
GrKurtosis	-0.15 (0.72)	1.31 (1.81)
GrNonZeros	0.75 (0.13)	0.79 (0.11)
RLM		
SRLE	0.87 (0.04)	0.90 (0.03)
LRLE	1.75 (0.39)	1.55 (0.24)
RLNU	1543 (526)	1508 (370)
GLNU	172 (89)	151 (53)
FractionRuns	0.83 (0.06)	0.86 (0.04)
GLCM		
AngScMom	0.012 (0.011)	0.010 (0.007)
Contrast	13.0 (6.9)	18.6 (9.7)
Correlation	0.58 (0.15)	0.49 (0.12)
Entropy	2.16 (0.30)	2.24 (0.24)
InvDfMom	0.33 (0.08)	0.30 (0.07)

*values are as given x 10^5

Abbreviations: Gr – Gradient, GrNonZeros – proportion of pixels with non-zero gradient, RLM – run-length matrix, SRLE – short run-length emphasis, LRLE – long run length emphasis, RLNU – run-length non-uniformity, GLNU – grey-level non-uniformity, FractionRuns – fraction of grey values occurring in runs, GLCM – grey-level co-occurrence matrix, AngScMom – angular second moment, InvDfMom – inverse difference moment.

Table 4. Summary of regression models

Parameter	Texture feature	B	SE(B)	Standardized Coefficient†	R^2	Adjusted R^2
BV.TV	Mean***	-1.1×10^{-4}	1.2×10^{-5}	-0.91		
	Entropy**	-0.5	0.1	-0.89		
	InvDfMom**	-1.2	0.4	-0.80		
	Variance***	1.7×10^{-7}	0.3×10^{-7}	0.52		
	Skewness***	0.11	0.02	0.48		
					0.81***	0.76***
Tb.Th	Mean***	-0.04	0.01	-0.55		
	Variance**	9.0×10^{-5}	3.0×10^{-5}	0.43		
	Skewness**	60	17	0.41		
	GLNU*	0.23	0.11	0.21		
					0.55***	0.47***
Tb.Sp	Mean***	0.27	0.02	1.17		
	GrMean***	-0.06	0.02	-0.76		
	Contrast***	19	5	0.72		
	Variance***	-4.0×10^{-4}	0.5×10^{-4}	-0.62		
	RLNU**	0.15	0.04	0.27		
					0.80***	0.75***
Tb.N	Mean***	0.15	0.02	0.63		
	GLNU***	1.3	0.4	0.38		
	GrVariance**	392	124	0.35		
					0.65***	0.60***

***p<0.001 **p<0.01 *p<0.05

†Standardized regression coefficient = 1 indicates an increase in 1 standard deviation of outcome variable for every 1 standard deviation increase in predictor variable

Abbreviations: SE – standard error, B – unstandardized regression coefficient, Abbreviations are otherwise as for table 3.